

A Study of Physical and Covalent Hydrogels Containing pH-Responsive Microgel Particles and Graphene Oxide

Zhengxing Cui,[†] Amir H. Milani,[†] Paula J. Greensmith,[†] Junfeng Yan,[†] Daman J. Adlam,[‡] Judith A. Hoyland,^{‡,§} Ian A. Kinloch,[†] Anthony J. Freemont,^{‡,§} and Brian R. Saunders^{*,†}

[†]School of Materials, The University of Manchester, Grosvenor Street, Manchester, M1 7HS, United Kingdom

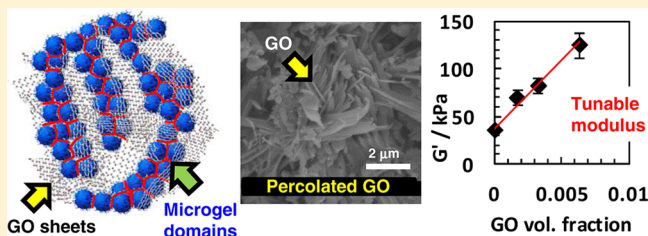
[‡]Centre for Tissue Injury and Repair, Institute for Inflammation and Repair, Faculty of Medical and Human Sciences, The University of Manchester, Oxford Road, Manchester, M13 9PT, United Kingdom

[§]NIHR Manchester Musculoskeletal Biomedical Research Unit, Manchester Academic Health Science Centre, Manchester, United Kingdom

Supporting Information

ABSTRACT: In this study we mixed low concentrations of graphene oxide (GO) with microgel (MG) particles and formed composite doubly cross-linked microgels (DX MG/GO) gels. The MG particles comprised poly(ethyl acrylate-*co*-methacrylic acid-*co*-1,4-butanediol diacrylate) with pendant glycidyl methacrylate units. The MG/GO mixed dispersions formed physical gels of singly cross-linked MGs (termed SX MG/GO), which were subsequently heated to produce DX MG/GO gels by free-radical reaction. The influence of the GO

concentration on the mechanical properties of the SX MG/GO and DX MG/GO gels was investigated using dynamic rheology and static compression measurements. The SX MG/GO physical gels were injectable and moldable. The moduli for the DX MG/GO gels increased by a factor of 4–6 when only ca. 1.0 wt % of GO was included. The isostrain model was used to describe the variation of modulus with DX MG/GO composition. Inclusion of GO dramatically altered the stress dissipation and yielding mechanisms for the gels. GO acted as a high surface area, high modulus filler and played an increasing role in load distribution as the GO concentration increased. It is proposed that MG domains were dispersed within a percolated GO network. Comparison of the modulus data with those published for GO-free DX MGs showed that inclusion of GO provided an unprecedented rate of modulus increase with network volume fraction for this family of colloid gels. Furthermore, the DX MG/GO gels were biocompatible and the results imply that there may be future applications of these new systems as injectable load supporting gels for soft tissue repair.



INTRODUCTION

The properties of hydrogels continue to evolve along with their structural complexity.¹ Remarkable improvements in gel modulus,² ductility,³ swelling ratios,⁴ and toughness⁵ have been achieved. While the majority of gels investigated have been constructed from small molecules, a new type of gel has recently emerged that is constructed solely from interlinked microgel (MG) particles.^{1,6} MGs are cross-linked polymer particles that swell in a good solvent^{7,8} or when the pH approaches the pK_a of the polyacid chains comprising the particles.^{8–10} Liu et al.⁶ showed that concentrated dispersions of pH-responsive MG particles containing pendant vinyl groups could be interlinked to form hydrogels, which are termed doubly cross-linked microgels (DX MGs). These hydrogels were constructed using sub-micrometer sized MG particles as the building blocks. They differ from other hydrogels containing MGs^{11,12} because MG particles act as both cross-linker and matrix element. If the MG particles were removed from our DX MGs, the gel would no longer exist, in contrast to hydrogels containing MGs. In this study we investigate DX

MGs prepared in the presence of low concentrations of graphene oxide (GO). GO, which is a high aspect ratio water-dispersible colloid, was used because it offered good potential for mechanical property enhancement. In this work we investigate and compare physical and covalent gels containing MG particles and GO. The aim of this study was to address two fundamentally important questions concerning the mechanical properties of the physical and covalent MG/GO composite gels. First, what is the stress transfer mechanism? Second, what is the strain dissipation mechanism?

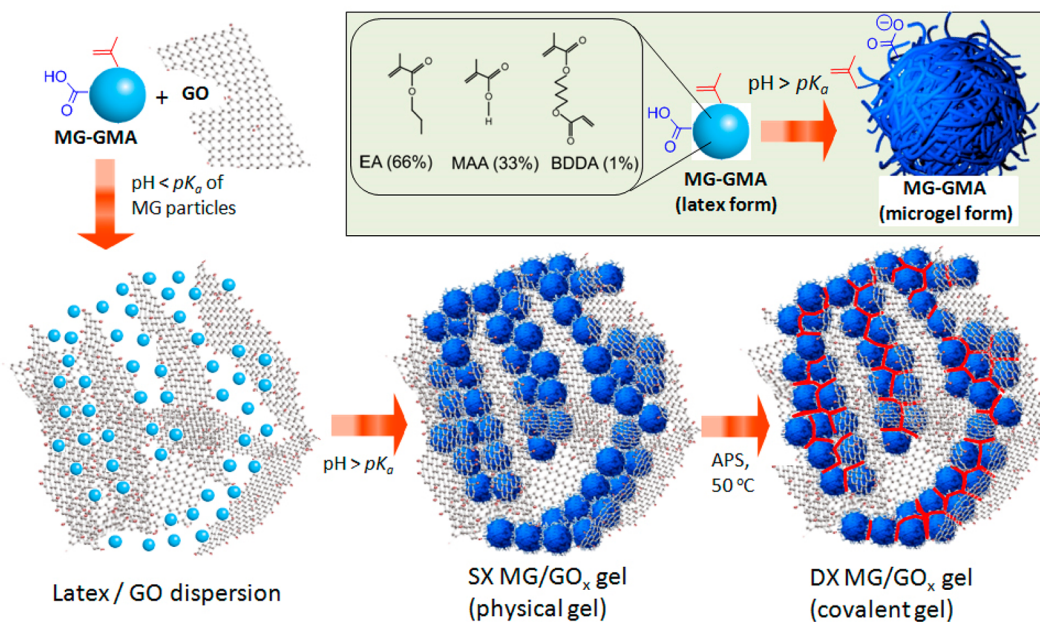
The DX MGs studied here were prepared using pH-responsive poly(ethyl acrylate-*co*-methacrylic acid-*co*-1,4-butanediol diacrylate) (poly(EA/MAA/BDDA)) MG particles functionalized with glycidyl methacrylate (GMA). These MG particles are abbreviated as MG-GMA. The MG particles swell from their collapsed, as-made, latex form with pH increase

Received: August 12, 2014

Revised: October 10, 2014

Published: October 14, 2014



Scheme 1. Depiction of the Preparation of DX MG/GO Gels^a

^aThe MG particles are prepared in their latex form and undergo pH-triggered swelling at pH values greater than their pK_a (inset). The latex was mixed with GO, and the pH increased to form a SX MG/GO physical gel. Heating the physical gel in the presence of ammonium persulfate (APS) covalently interlinked neighboring MG particle interfaces (shown in red) to form a DX MG/GO gel. The MG phase is proposed to exist as domains within percolated, exfoliated, GO sheets.

(Scheme 1), and this process transforms a low viscosity fluid into a shear-thinning physical gel. The MG-GMA particles were then subjected to free-radical coupling via pendant vinyl groups (from GMA).⁶ The term DX is used to identify that two types of cross-linking were present. Besides the covalent *intraparticle* cross-linking (within singly cross-linked (SX) MGs), we introduced a second (doubly) covalent *interparticle* cross-linking that interlinked the MG particles. The latter transformed the shear-thinning (injectable) gel into an elastic, permanently cross-linked, hydrogel of interlinked MG particles. In Scheme 1 the interlinking is identified with red interfaces. DX MGs have potential application as injectable gels for the restoration of the mechanical properties of degenerated intervertebral discs (IVDs).¹³

Many of the design rules governing the mechanical properties of DX MG gels have become clear since their first report in 2011.⁶ The modulus of DX MG gels has contributions from both *intraparticle* and *interparticle* cross-links.⁶ Because the precursor is a physical gel of swollen MG particles, close contact between vinyl groups on neighboring MG particles is essential for interparticle cross-linking and DX MG formation. Highly cross-linked MG particles show low pH-triggered swelling¹⁴ which can lead to the paradoxical situation where high modulus MG particles lead to low modulus DX MGs because of poor inter-MG cross-linking. The modulus of DX MGs increases with MG particle concentration,⁶ which provides a simple mechanical property tuning method. At fixed MG particle concentration the modulus can also be increased by increasing the extent of pendant vinyl functionalization of the MG particles.^{6,15} Here, we investigated the effect of GO concentration on the mechanical properties of DX MG/GO composites at constant MG particle concentration and extent of vinyl functionalization.

Graphene has outstanding mechanical, electrical, and thermal properties.^{16–20} GO is rich with hydrophilic groups on the

surface and at the edge of the sheets.²¹ Moreover, GO is readily water-dispersible.¹⁶ The hydrophilic groups comprise hydroxyl, carboxyl, epoxy, and ketone groups, and the Lerf–Klinowski model is currently the most widely accepted structural model for GO.¹⁸ Furthermore, GO has received a great deal of attention because of its high aspect ratio, high modulus,²² and ability to be blended with polymers and incorporated in gels.^{23–25} The biological applications of GO have also been actively investigated,^{26–28} and there is good potential for GO use *in vivo*.²⁹ Here, we investigate colloidal gel composites containing GO as a mechanical reinforcement colloid. Although the major potential application of our DX MG/GO gels is for repairing load supporting tissues, we do not focus on this application in this study. Rather, we concentrate on establishing structure–mechanical property relationships for the new gels studied.

The starting point for composite gel preparation (Scheme 1) was a mixed dispersion of vinyl-functionalized MG particles in latex form and GO. A pH increase caused pH-triggered swelling of the MG-GMA particles and formation of a physical gel, termed SX MG/GO_x, where x is the total concentration of GO added in wt %. As will be shown, the physical gels were moldable and injectable. When heated in the presence of initiator (ammonium persulfate, APS), the MG-GMA particles covalently interlinked and DX MG/GO_x gels were formed. Our DX MG/GOs differ considerably from other reported hydrogel/GO composites^{30–36} because we used preformed MG particles to form the hydrogel. These are macroscopic composite gels constructed from colloidal scale building blocks. Uniquely, our approach does not use small monomers.

In this study the morphology and properties of SX MG/GO and DX MG/GO composite gels are reported for the first time. The gels are explored using dynamic rheology and compression measurements, and their morphology is assessed using SEM. The modulus is found to obey the isostrain biphasic model of

Morris,³⁷ which is the first report of this behavior for hydrogels containing GO to our knowledge. Further, our data point to a structural model in which the MG particles exist as domains within a percolated GO network. While the GO is not believed to be covalently linked to the DX MG phase, there is very good stress transfer via the GO sheets. The addition of 1 wt % of GO is shown to increase the modulus by a factor of 6 and dramatically change strain dissipation. Moreover, the inclusion of GO is shown to dramatically increase the modulus compared to earlier reports for pure DX MGs. The very good modulus tunability afforded by these new biocompatible injectable composite gels offers potential for future application in the context of repairing load supporting soft tissue.

EXPERIMENTAL DETAILS

Materials. Graphite (Graphexel grade 2369), EA, MAA, BDDA, GMA, H₂SO₄, NaNO₃, NaOH, potassium permanganate, H₂O₂, APS, phosphate buffered saline (PBS, pH = 7.4 bioreagent), and N,N,N',N'-tetramethylethylenediamine (TEMED) were all purchased from Sigma-Aldrich. All reagents were the highest purity available and used as received. Biological reagents were prepared using Dulbecco's modified Eagle's medium (DMEM, Gibco), fetal bovine serum (FBS, Gibco), and antibiotic/antimycotic (Sigma-Aldrich). All water was of ultrahigh purity and was distilled and deionized.

Synthesis of Graphene Oxide. Preparation of GO was conducted using a modified Hummers method.³⁸ Graphite powder (5 g) was introduced in concentrated H₂SO₄ (170 mL) with stirring. An ice bath was used to cool the mixture. NaNO₃ (3.75 g, 0.04 mol) was added and stirring continued for 5 h. Potassium permanganate (25 g, 0.16 mol) was gradually added at a rate that prevented the temperature of the mixture exceeding 20 °C. After all of the additives were dissolved, the ice bath was removed and the temperature was increased to 35 °C using heating with stirring for 2 h. The dispersion was then stirred at room temperature for 7 days. To obtain exfoliated GO, the product was slowly dispersed into 550 mL of 5 wt % H₂SO₄ solution and stirred for 3 h. Then, aqueous H₂O₂ (15 g, 30 vol %) was slowly added over a period of 5 min. The mixture became a gold colored dispersion, and stirring was continued for a further 2 h. The suspension was diluted with 500 mL of 3 wt % H₂SO₄ solution containing 0.5 wt % H₂O₂ and left overnight. The product was centrifuged at 9000 rpm for 20 min, and the clear supernatant liquid was removed. The remaining viscous liquid was washed with a further 500 mL of 3 wt % H₂SO₄/0.5 wt % H₂O₂ solution. The washing process was repeated nine times, and then the mixture was further purified by dialysis for 7 days. The final pH of the purified, exfoliated, GO dispersion was 7.2.

Synthesis of Poly(EA/MAA/BDDA) Microgel. The synthesis of this MG was conducted using the seed-feed emulsion polymerization method according to a previously published method³⁹ and is briefly described here. The MG particles contained about 33 wt % of MAA with respect to total monomer. A comonomer solution (250 g) containing EA (167 g, 1.88 mol), MAA (83 g, 0.83 mol), and BDDA (2.5 g, 0.01 mol) was prepared. A total of 31.5 g of the comonomer solution was used for the seed formation. The latter solution was added to water (518 g) containing SDS (1.8 g, 0.006 mol), and then K₂HPO₄ (3.15 g of a 7 wt % aqueous solution) and APS (10 g of a 2 wt % solution) were added. The seed was prepared at 80 °C with mechanical stirring under nitrogen for 30 min. Then the remaining monomer solution was added at a uniform rate over a period of 1.5 h. The reaction was continued for further 2 h. The product was purified by extensive dialysis using water.

Synthesis of GMA-Functionalized Poly(EA/MAA/BDDA) Microgel. MG dispersion (100 g of 10 wt % dispersion) was mixed with GMA (16.6 g, 0.12 mol). The pH of the mixture was adjusted to 5.4 using aqueous NaOH solution (0.05 M). The mixture was heated at 50 °C for 8 h. After reaction, chloroform was used to wash the product and then removed using rotary evaporation and the process repeated. The MG-GMA dispersion was then dialyzed extensively.

Preparation of SX MG/GO Physical Gels and DX MG/GO Covalent Gels. To prepare the composite gels a thoroughly mixed dispersion containing MG-GMA and GO was first prepared at a pH of about 4.7. As an example, the DX MG/GO_{1.0} composite was prepared from mixing MG-GMA (6.67 g of 15 wt % dispersion) and GO (22.22 g of 0.45 wt % dispersion). (For the other DX MG/GO_x systems the masses of GO were reduced accordingly.) The mixed dispersion was concentrated to ~10 g using rotary evaporation at room temperature. An aqueous solution (0.2 g) of APS and NaOH was then added with stirring. The added solution contained 3.4 wt % of APS, and the concentration of NaOH was 4 M. The gel had a final pH of ~7.2. This process triggered formation of an SX MG/GO physical gel. To form the DX MG/GO gel the SX MG/GO mixture was heated at 50 °C for 8 h. (For the two demonstration gel preparations where TEMED was present, the covalent interlinking reaction was conducted at 37 °C using an overall TEMED concentration of 0.08 M.) All the gels studied in this work contained a MG particle concentration of 10 wt % and the pH values were adjusted to ~7.2. The SX MG/GO physical gels were studied in the absence of added APS.

Physical Measurements. Titration measurements were performed using a Mettler Toledo DL 15 titrator in the presence of aqueous 0.1 M NaCl. TGA measurements were performed using a TA Instruments Q500 with a heating rate of 10 °C/min. Photon correlation spectroscopy (PCS) measurements were performed using a BI-9000 Brookhaven light scattering apparatus (Brookhaven Instrument Cooperation) equipped with a 20 mW HeNe laser, and the detector was set at a scattering angle of 90°. TEM data were obtained using a JEOL JEM-2011F operating at an accelerating voltage of 200 kV. Zeta potential data were obtained using a Malvern Nano ZS using a GO concentration of 0.01 wt % and a background electrolyte concentration (NaNO₃) of 0.01 M. The rheological properties of the gels were measured using a TA Instruments AR-G2 temperature-controlled rheometer equipped with an environmental chamber. The measurement geometry used a 20 mm flat disk. Frequency-sweep and strain-sweep data were measured at 25 °C. For the frequency-sweep data a strain of 1% was used. The strain-sweep data were measured using a frequency of 1 Hz. The compression tests were conducted using an Instron series 5569 load frame equipped with a 100 N load cell. The compression rate was 2 mm/min, and the average height and diameter of the gel cylinders were 10.8 mm and 9.6 mm, respectively. Modulus values were calculated from the initial gradient of stress-strain curves at strains (ϵ) of less than 10%. Data are also shown in terms of the extension ratio λ ($= 1 - \epsilon$). SEM measurements were obtained using a Philips xl30 instrument. Before observation, gel samples were rapidly freeze-dried using liquid nitrogen. The SEM samples were coated with platinum prior to examination.

Assessment of Cytotoxicity. Human nucleus pulposus (NP) cells were cultured in Dulbecco's modified Eagle's medium supplemented with 10% fetal bovine serum and antibiotic/antimycotic at 37 °C in a humidified 5% CO₂ atmosphere. Cells were harvested by trypsinization and seeded at a density of 2×10^4 cells/well into 24-well culture plates containing 13 mm diameter sterile glass coverslips. After 24 h in culture, sterile toroid-shaped composites (see inset of Figure 7a) were introduced into wells and cultured for a further 10 days. After this time the coverslips were removed and cell viability assessed by live/dead assay (Invitrogen, U.K.). Images were taken with an Olympus BX51 fluorescence microscope and Leitz Diavert inverted light microscope.

RESULTS AND DISCUSSION

Microgel and Graphene Oxide Characterization. The GMA-functionalized poly(EA/MAA/BDDA) MG (abbreviated as MG-GMA) was prepared by seed-feed emulsion polymerization and subsequently vinyl-functionalized by reaction with GMA (see Experimental Details). The extent of GMA functionalization and the apparent pK_a were determined to be 3.0 mol % and 6.6, respectively, from titration data (see Figure S1 and Table S1 in the Supporting Information). The MG-GMA particles were spherical (Figure S2a in the

Supporting Information) with a number-average diameter ($d_{n(\text{SEM})}$) of 108 nm (coefficient of variation = 16%). The MG-GMA particles were pH-responsive (Figure S2b in the Supporting Information) and had a hydrodynamic diameter (d_h) of 120 nm at pH = 4. We assume that the particles at this pH were fully collapsed because the latter diameter was close to $d_{n(\text{SEM})}$. With increasing pH the MG-GMA particles exhibited pH-dependent swelling with a d_h value of \sim 307 nm at pH = 7.2 ($d_{h(7.2)}$). At higher pH values the value for d_h was constant. A MG-GMA particle volume swelling ratio ($Q = (d_{h(7.2)}/d_{h(4.0)})^3$) of 16.7 was calculated from the data. The MG-GMA particles swelled considerably in the vicinity of pH = 7.4. The latter pH is a common target for biomaterial applications.

The GO used in this study was prepared by a modified Hummers method (see Experimental Details). A representative TEM image for GO is shown in Figure S2c in the Supporting Information, and a folded sheet is evident. A representative SEM image (Figure S2d in the Supporting Information) indicated an average sheet diameter of about 2 μm , which agrees with the approximate diameter of the equivalent disk. The Raman spectrum for GO differs considerably from that of graphite (Figure S3 in the Supporting Information) and is typical of that reported for GO⁴⁰ with the G band at \sim 1600 cm^{-1} and the D band at \sim 1350 cm^{-1} . Both of the bands had similar intensities. The zeta potential measured for GO at pH = 7.2 was -63.5 mV. The combination of these properties is consistent with those reported for GO in the literature.^{20,41,42}

Probing Stress Transfer and Dissipation of Gels Containing Graphene Oxide. DX MG/GO gels were prepared by mixing MG-GMA and GO dispersions, increasing the pH, and then heating (see Scheme 1). At pH = 4.3, which is less than the pK_a for the MG-GMA particles (Table S1 in the Supporting Information), the SX MG/GO dispersions were free-flowing (see Figure 1a). A fluid-to-gel transition for the

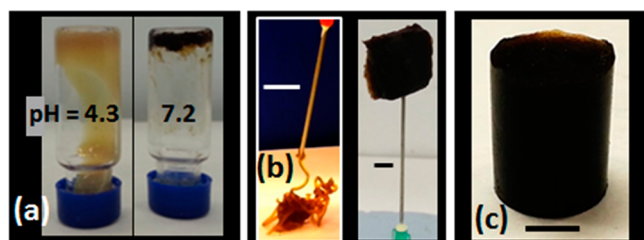


Figure 1. Formation and behaviors for SX MG/GO and DX MG/GO gels. The pH-triggered fluid-to-gel transition is shown in panel a using SX MG/GO_{0.50} as an example. The SX MG/GO gels were injectable and also moldable as can be seen from the SX MG/GO_{1.0} gel images shown in panel b. DX MG/GO gels were prepared as cylinders and a DX MG/GO_{1.0} gel is shown in panel c. The scale bars for panels b and c are 5 mm.

mixed SX MG/GO dispersion was triggered by increasing the pH to 7.2 (Figure 1a). In this state the swollen MG particles occupied most of the volume and prevented translation of nearest-neighbor MG particles (and GO) due to excluded volume effects. The SX MG/GO dispersions formed gels at pH of 7.2 that were shear-thinning and could be injected through a narrow gauge syringe needle (Figure 1b). Injectability is a potentially useful property for a load-bearing gel in the context of soft tissue repair.^{13,43} While colloidal gels have previously been reported that formed moldable macroscopic gels due to heteroaggregation,⁴⁴ the present gels did not require hetero-

aggregation, but simply a pH change and the presence of a minor proportion of GO. It can be seen from Figure 1b that these physical gels could be molded into self-supporting shapes. The ability to form SX MG/GO gels into self-supporting shapes and cure them using covalent interlinking provides the first example of “shape and set” GO-based colloidal composite gels to our knowledge. We note that pure GO dispersions are also known to form gels⁴⁵ and images of tubes containing different GO concentrations (C_{GO}) for this study are shown in Figure S4 in the Supporting Information. We show below that inclusion of MG particles increased gel modulus.

The frequency-sweep dynamic rheology data for GO, SX MG/GO, and DX MG/GO gels are shown in Figure 2a–c. The GO data are included as a control. The values for the storage modulus (G') are greater than those for the loss modulus (G'') over the whole frequency range studied for all systems, showing that each was a viscoelastic solid. The frequency dependencies for G' and G'' are generally low for each gel. The G' values scale with frequency ($=\omega/2\pi$, ω is the oscillation frequency) according to $G' \sim \omega^{n'}$,⁴⁶ where n' is the frequency exponent. The value for n' approaches zero as the relaxation time becomes longer than the experimental time and the rigidity increases. Figure 2d shows values for n' plotted as a function of C_{GO} . The value for n' decreases in the order GO > SX MG/GO > DX MG/GO. It follows that the relaxation times increase in the same order. The presence of MG particles (for SX MG/GO) and their covalent interlinking (for DX MG/GO) decreased the ability of the stress distributing elements to become disconnected within the experimental times probed by these oscillatory rheology measurements. Accordingly, we propose that the covalent interlinking of the MG particles (for DX MG/GO) restricted the freedom of the GO sheets to move in response to strain.

The value for G' can be considered as a measure of network connectivity. According to Figure 2e the connectivity of the networks increased with C_{GO} for all of the gels. (It will be shown in Figure 3 that the increase of G' is linear with respect to C_{GO} .) In the case of SX MG/GO, the increased connectivity arises from the swollen MG particles, which form a space-filling physical gel, and stress transfer occurs between the MG particles and the GO sheets. The fact that the G' values for the DX MG/GO gels are higher than those for the respective SX MG/GO shows that the double cross-linking contributed additional elastically effective chains. It is proposed that the covalent interlinking of the MG particles more effectively trapped the GO sheets in their positions within the DX MG/GO gels.

The values for G'' and G' provide measures of the energy dissipated and stored, respectively, per unit strain.⁴⁷ Hence, as the value for $\tan \delta (=G''/G')$ increases, the proportion of energy dissipated by the gel under strain also increases. This is greatest for the GO gels (Figure 2f). It follows that the GO sheets were least constrained for the GO gels and they were not strongly linked together. This suggestion is consistent with the literature for GO where the principal attractive interactions are hydrophobic attraction and hydrogen bonding,^{48,49} both of which are relatively weak (and reversible) compared to covalent bonds.

Compared to the GO gels, inclusion of non-interlinked MG particles (SX MG/GO) greatly decreased $\tan \delta$ (Figure 2f), and this was further decreased by MG interlinking (for DX MG/GO). The physical and covalently interlinked MG particle matrixes were both effective in decreasing dissipation and are

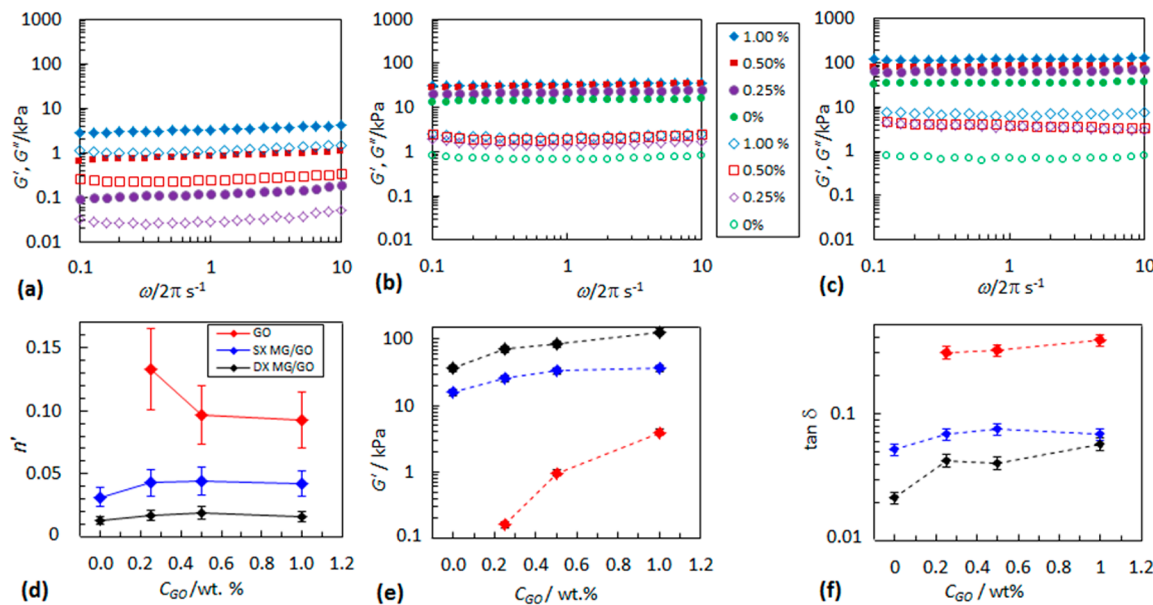


Figure 2. Frequency-sweep data for various gels containing GO. The variation of G' (closed symbols) and G'' (open symbols) with frequency ($\omega/2\pi$) is shown for GO (a), SX MG/GO (b), and DX MG/GO (c). The legend for panel b also applies to panels a and c (ω is the oscillation frequency in rad s^{-1}). Panel d shows the frequency exponent (n') dependence on GO concentration (C_{GO}). Panel e shows the variation of G' with C_{GO} . Panel f shows the variation of $\tan \delta (=G''/G')$ with C_{GO} . The error bars for some of the points in panel e are smaller than the data points. The legend for panel d also applies to panels e and f.

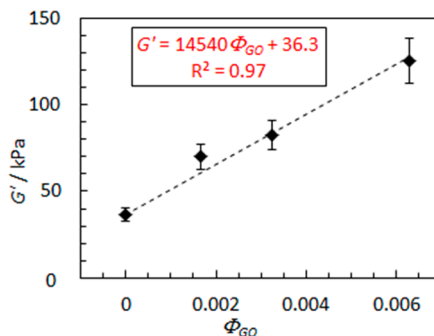


Figure 3. Variation of modulus with GO content for DX MG/GO gels. Dependence of storage modulus (G') on the volume fraction of GO. The values for G' used here were measured at 10 Hz. It should be noted that Φ_{GO} is proportional to C_{GO} .

proposed to have greatly restricted the ability of the GO sheets to move in response to strain. It is noteworthy that $\tan \delta$ was much lower for the (GO-free, $C_{GO} = 0$) DX MG gel (Figure 2f) compared to the DX MG/GO gels. Accordingly, the exfoliated GO sheets caused a greater degree of movement within the DX MG/GO gels (and hence dissipation) in response to strain. This trend is opposite to that expected if the GO sheets were covalently linked to the network because in that case less dissipation would be expected. Free-radical cross-linking of GO has been proposed for other GO hydrogel composites.^{35,36} In the present case our data suggest that the GO sheets were *not* covalently linked to the interlinked DX MG particle matrix. While we cannot be certain that covalent cross-linking between the DX MG and GO phases was completely absent, substantial interphase cross-linking would be expected to result in a more rigid network compared to the parent DX MG gel, with similar or lower $\tan \delta$ values. The $\tan \delta$ increase with increasing C_{GO} (Figure 2f) is further support for the absence of significant interphase cross-linking.

The DX MG/GO gels contained covalently interlinked MG particles as evidenced by the fact that they did not redisperse when placed in water for extended periods. The GO phase can be viewed as a reinforcing, high modulus filler. In this context the percolation concentration for GO is important. Because the rheology data showed that the GO dispersions were gels (Figure 2a), it is reasonable to conclude that the percolation concentration for GO was less than 0.25 wt %. This conclusion is in agreement with the study of Vasu et al.⁴⁵ Consequently, we tested a model for the DX MG/GO composites consisting of a relatively low modulus (MG) phase dispersed within a high modulus phase (GO). Under these conditions the biphasic isostrain model of Morris³⁷ should apply. The isostrain model assumes that the modulus of the composite is the volume fraction weighted sum of the modulus values for each component. This model was tested using the following equations.

$$G' = G'_{GO}\Phi_{GO} + G'_{DX MG}\Phi_{DX MG} \quad (1)$$

$$G' = G'_{DX MG} + \Phi_{GO}(G'_{GO} - G'_{DX MG}) \quad (2)$$

For the above equations G'_{GO} and $G'_{DX MG}$ are the storage moduli for GO and DX MG, respectively. We used Φ_{GO} and $\Phi_{DX MG}$ for the volume fractions of GO and DX MG gel networks on a dry weight basis as we could not be certain of the actual volume fractions occupied by each phase in the gels. Equation 2 was obtained using the assumption $\Phi_{GO} + \Phi_{DX MG} = 1$. We further assumed that the density of the dry MG particles⁶ and GO²² was 1.2 and 1.8 g cm^{-3} , respectively. Figure 3 shows that the G' vs Φ_{GO} data were linear and could be fitted using eq 2 and a $G'_{DX MG}$ value of 36.3 kPa (from Figure 2e). The data imply that there is good potential to *dial up* the modulus of these composite GO-based gels using composite formulation. Using the gradient and eq 2, a value of G'_{GO} of 14.6 MPa was calculated. Dikin et al.²² reported a tensile modulus of 32 GPa for “GO paper”, which is four orders of

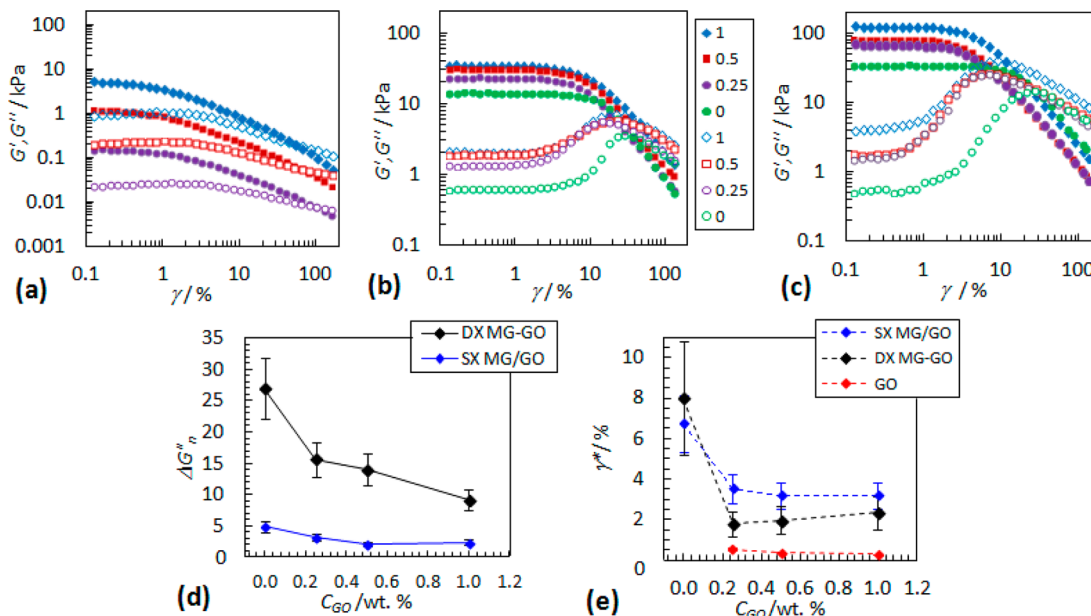


Figure 4. Strain-sweep data for various gels containing GO. The variation of G' (closed symbols) and G'' (open symbols) with strain (γ) are shown for GO (a), SX MG/GO (b), and DX MG/GO (c). The legend for panel b also applies to panels a and c. Panel d shows the $\Delta G''_n$ (see text) dependence on GO concentration (C_{GO}). Panel e shows the variation of the yield strain (γ^*) with C_{GO} .

magnitude higher than G'_{GO} . The reason why G'_{GO} is much lower than the modulus value from Dikin et al. is that the GO sheets were dispersed within a gel and had some freedom to move under strain. The interactions that transferred stress between the GO sheets and DX MG domains most likely involved water-mediated hydrogen bonding and also reversible hydrophobic interactions. It is not surprising that these interactions, which are reversible and dissipative, are less efficient for load transfer compared to those present for GO paper.²²

Strain-sweep dynamic rheology measurements are well suited to probe strain-induced failure mechanisms for gels. The GO gels (Figure 4a) had low ductility in that G' decreased at strains greater than about 0.2%. This tendency for G' to decrease at low strain for GO gels was reported by Vasu et al.⁴⁵ The GO gels showed only weak G'' maxima, and both the G' and G'' data decreased strongly with increasing strain. This behavior contrasts to SX MG/GO (Figure 4b) and DX MG/GO gels (Figure 4c) where the G' values remained constant until much higher strain values were reached and strong maxima for G'' are evident. The maxima for the MG-containing gels are attributed to cage breaking⁵⁰ and are largest for the DX MG/GO gels. This trend can be seen more clearly in Figure 4d, where $\Delta G''_n$ ($= (G'' - G''_{min})/G''_{min}$) is plotted as a function of C_{GO} . (G''_{min} is the minimum G'' value in the linear viscoelastic region, i.e., at the lowest strain.) The use of $\Delta G''_n$ normalizes the G'' maxima⁵¹ and show that inclusion of GO progressively decreased the relative magnitude of the G'' maximum. The extent of cage breaking during dissipation is proposed to be diminished by GO inclusion. This conclusion would follow from a percolated structure where MG domains are increasingly separated by GO sheets (see Scheme 1) and the behavior occurred when the GO concentration was as low as 0.25 wt %.

Applying the general approach used elsewhere for brittle viscoelastic solids,⁵² we define a yield strain (γ^*) corresponding to the γ value where the initial modulus had decreased significantly. In the present study a 10% modulus decrease was

used. The value of γ^* corresponds to a point where 90% of the network connectivity was intact. (Higher static yield strains were measured using compression measurements; Figure 6.) The data from Figure 4e show that the GO gels were brittle, which is due to the percolated network of stiff GO sheets. Inclusion of GO within the SX MG/GO gels increased γ^* substantially compared to the GO gels and therefore improved the ductility of the GO network. We suggest that the MG particles separated GO sheets and opposed breaking of network connections under strain due to their swollen state, which restricted excessive GO sheet movement.

For the DX MG/GO gels covalent interlinking of the MG particles decreased the γ^* values and hence the ductility (Figure 4e) compared to the SX MG/GO gels. This is expected due to a decreased ability of the MG particles to move under an imposed strain due to covalent inter-MG linking. Overall, the γ^* data reveal that inclusion of GO dramatically changed the dissipation and yielding behavior of the composite gels compared to the GO-free ($C_{GO} = 0$) SX MG and DX MG gels. Generally, the SX MG/GO and DX MG/GO became more like the GO gels in terms of stress dissipation and yielding behaviors. These data are congruent with our proposal that the gels consist of a percolated GO network containing MG particle domains.

DX MG/GO Morphology, Static Mechanical Properties, and Biocompatibility. In this part of the study we focus on the properties of DX MG/GO gels because they have the most promising properties for future biomaterial application, e.g., as load supporting injectable gels for IVD repair.¹³ A detailed study of the potential for application of the SX MG/GO and DX MG/GO gels will be presented in future work. Here, we focus on the fundamental aspects of structure–property relationships and also present preliminary biocompatibility data. Because the gels investigated here were prepared at 50 °C (which is too high for use *in vivo*), they could only have potential future use in humans after being injected into molds. However, we note that introduction of an accelerator enabled

the DX MG interlinking temperature at 37 °C,¹³ and this approach is expected to be suitable for our DX MG/GO gels. To test this proposal two demonstrator DX MG/GO gels were prepared at 37 °C in the presence of TEMED and the mechanical properties probed by dynamic rheology. The DX MG/GO_{0.5} and DX MG/GO_{1.0} gels cured within about 20 min, and the strain-sweep data were similar to those for the respective gels prepared at 50 °C (see Figure S5 in the Supporting Information). The remainder of the study focuses on gels prepared at 50 °C in the absence of added TEMED.

The morphology of the freeze-dried DX MG-GO gels was probed by SEM. Figure 5a shows a freeze-dried image for a DX

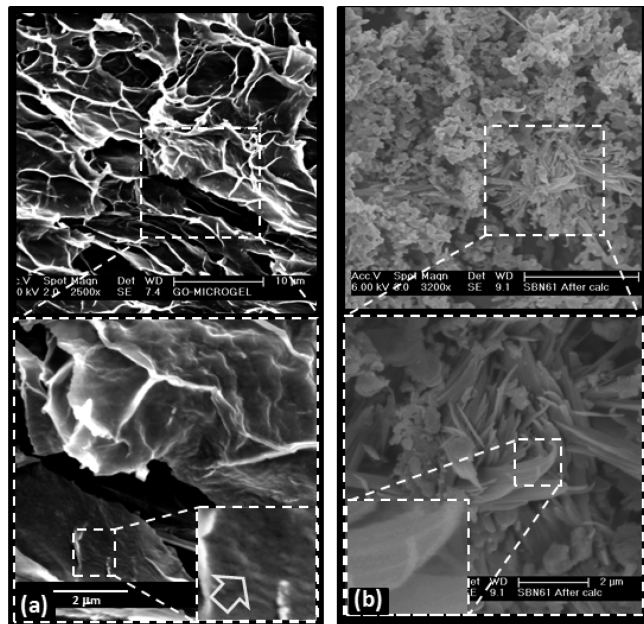


Figure 5. DX MG/GO_{1.0} gel morphology. Images are shown for DX MG/GO_{1.0} before (a) and after (b) being heated to 550 °C under a N₂ atmosphere. The inset for panel a shows that MG particles could be seen (arrow). The inset for panel b shows GO sheets.

MG/GO_{1.0} in the as-made state. The morphology was porous and typical of that reported for conventional hydrogel/GO composites.^{31,36,53} For our DX MG/GO gels, spherical MG particles can be seen from the inset of Figure 5a (arrow). However, the GO sheets were less clear. In order to reveal the GO sheets a freeze-dried DX MG/GO_{1.0} hydrogel was heated at 550 °C under N₂ for 1 h. This process was conducted

because GO has superior thermal stability to conventional polymers.⁵⁴ The heating process resulted in the freeze-dried mass content decreasing by 90% (see TGA data in Figure S6 in the Supporting Information). SEM images (Figure 5b) show that the GO sheets became exposed. Not all of the GO sheets were exposed because significant, degraded, DX MG remained. Nevertheless, the exposed GO sheets can be seen to have a space-filling morphology. This morphology generally supports our proposal that GO formed a percolated network throughout the DX MG/GO gels. Because the DX MG/GO gels were prepared by interlinking SX MG/GO gels (without further mixing), it is reasonable to infer that the morphology of the SX MG/GO gels was similar to that of the DX MG/GO gels (Figure 5).

Static compression stress vs extension ratio data were measured for the DX MG/GO gels (Figure 6a). The inclusion of GO decreased the maximum strain (ϵ_{\max}) (Figure 6b) when the data for the DX MG/GO gels are compared to that for DX MG ($C_{GO} = 0$). For the DX MG/GO gels, the ϵ_{\max} values (and hence ductility) were not significantly dependent on C_{GO} despite the major increase in the maximum true stress values that occurred ($\sigma_{\max(T)}$, Figure 6b). The fact that the ϵ_{\max} values for DX MG/GO were not distinguishable and were all significantly lower than for the GO-free DX MG (Figure 6b) confirms the trend for the γ^* values that was apparent from strain-sweep rheology (Figure 4e). These data support our assertion that a major change in the gel architecture occurred upon inclusion of GO within DX MG/GO. The values for ϵ_{\max} were about 25%, and these are potentially useful in the context of an injectable gel for IVD repair because the axial regional compressive strains experienced within the IVDs of humans are much less than 10%.⁵⁵

The values for the modulus, E , were calculated from the gradients of the stress-strain curves and are shown in Figure 6c. A linear relationship between E and C_{GO} is evident, which is the same general trend established from rheology experiments (Figure 3). These data show that it should be straightforward to tune the modulus of the DX MG/GO gels through control of C_{GO} , which could be useful in the context of IVD repair.¹³ The maximum E value was 300 kPa, which is an impressive value for a gel containing a high water content (89 wt %). It is remarkable that E increased by a factor of 6 while the increase in network forming material (i.e., GO) accounted for only an additional 1 wt %. This major increase in the modulus achieved through addition of low GO concentration is in agreement with trends reported elsewhere for sugar-based aqueous gels, where

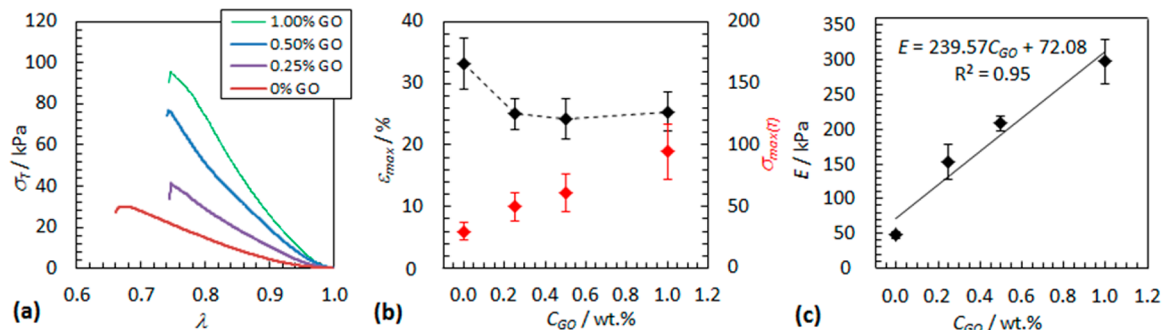


Figure 6. Static compression data for various DX MG/GO gels. Panel a shows true stress (σ_T) vs extension ratio (λ) curves for different DX MG/GO gels. Panel b shows the effects of GO concentration on the maximum strain (ϵ_{\max}) and maximum true stress ($\sigma_{\max(T)}$). The variation of modulus with C_{GO} is shown in panel c.

functionalized GO was used.⁵⁶ However, for the present gels functionalization of GO was not required.

As the DX MG/GO gels have potential future application in the context of IVD repair, we conducted a preliminary biocompatibility study. The biocompatibility of DX MG/GO_{0.5} gels was investigated by culturing human NP cells in direct contact with composites for 10 days, and cell viability was assessed by live/dead assay (Figure 7). Annular DX MG/GO_{0.5}

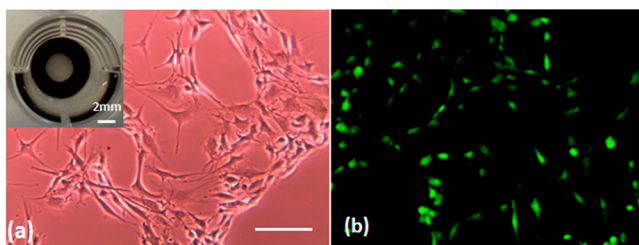


Figure 7. Cell challenge experiments for DX MG/GO gels. Nucleus pulposus cells contacted DX MG/GO_{0.5} under a toroid-shaped gel (inset of panel a) and had a normal elongated morphology. (b) Live/dead assays after 10 days showed that cells remained viable in contact with the gel. The scale bar represents 100 μm and applies to panels a and b.

composites (inset of Figure 7a) were introduced into 24-well culture plates containing cultures of human NP cells on glass coverslips. Live cells in the assay are distinguished by the presence of calcein (green), whereas dead cells are stained with ethidium homodimer-1 (red). Figure 7a shows the adherence and morphology of NP cells in culture with the DX MG-GO_{0.50} composite. The morphology was indicative of viable NP cells. Figure 7b shows live/dead assay fluorescent microscopy images of NP cells in contact with the gel, and a very high proportion of live cells were evident (greater than ca. 95% from our images). It follows that there was a high proportion of viable, adherent NP cells present after 10 days of culture in direct contact with DX MG/GO_{0.50}. The DX MG/GO gel had good biocompatibility under the conditions studied. These trends match those established earlier for GO-free DX MGs.¹³

Proposed Morphology for SX MG/GO and DX MG-GO Gels and Roles of Each Component. Our MG particles aided GO dispersion (Figure 1a), which is consistent with the reported amphiphilic nature of GO¹⁶ and related MG particles.⁵⁷ The MG particles are proposed to have physically adsorbed onto the GO sheets via hydrophobic and hydrogen bonding interactions. The subsequent pH-triggered MG particle swelling increase caused physical gel formation (Figure 1a,b); when heated, MG particle interlinking gave DX MG/GO gels (Figure 1c). The depictions for the SX MG/GO and DX MG/GO gels shown in Scheme 1 capture the key morphological features. In each case exfoliated GO sheets separate domains of MG particles which are either sterically confined (SX MG/GO) or covalently interlinked (DX MG/GO). The GO sheets, which form a percolated network throughout the gels, occupy a much smaller volume fraction than depicted in Scheme 1. (The proportion of MG particles shown was decreased for clarity.) Because the tan δ values of the DX MG/GO gels were higher than for the parent DX MG (Figure 2f), it is proposed that cross-linking did not occur to a significant extent between the DX MG and GO phases.

Considering the mechanical properties of the DX MG/GO gels, the GO sheets acted as a high modulus rigid filler. The

adsorbed MG particles transferred load between neighboring GO sheets via the DX MG domains that occupied inter-GO spaces, i.e., GO-to-DX MG-to-GO load transfer. Because of their space-filling nature, the MG particles effectively lock the GO sheets in place until a critical yield strain is reached. The high swelling pressure of the DX MG phase opposed the large scale strain-induced GO sheet alignment required for yielding of pure GO gels.⁴⁵ Hence, the role of the MG particles was to provide an effective load transfer mechanism between the GO sheets and an energetic barrier to their strain induced alignment. The role of the GO was to provide a high modulus continuous phase which increasingly distributed load as the total GO surface area increased. The latter increased with increasing C_{GO}.

Mechanical Property Comparison of GO-Free and GO-Containing SX MG and DX MG Gels. Although a range of SX MGs and DX MGs have been reported,^{6,13,58} like conventional gels, moderate increases in polymer concentration are required to substantially increase G'. Figure 8 shows a

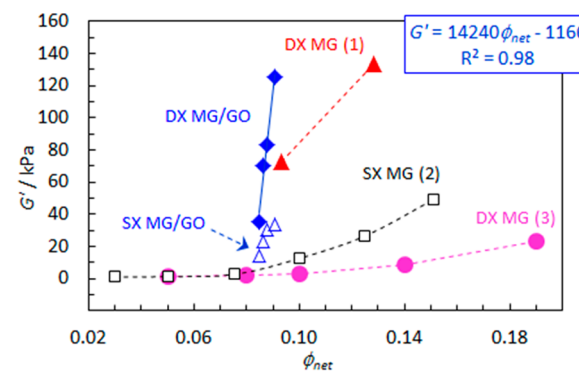


Figure 8. Modulus variation with network concentration for SM MG and DX MGs. The effects of network volume fraction (ϕ_{net}) on the storage modulus (G') for various MG-based gels are shown. The data for DX MG/GO and SX MG/GO are from this study. A line of best fit is shown for the DX MG/GO gels. The sources for the other DX MG and SX MG data are as follows: 1 = poly(MMA/MAA/EGDMA);¹³ 2 = poly(EA/MAA/BDDA);⁵⁸ 3 = poly(MMA/MAA/EGDMA).⁶ The dashed lines are guides to the eye. MMA and EGDMA are methyl methacrylate and ethylene glycol dimethacrylate.

comparison of the reported G' values for DX MGs and SX MGs for a range of network volume fractions (ϕ_{net}). The network comprises polymer from the MG particles for conventional SX MGs and DX MGs, or polymer and GO for SX MG/GO and DX MG/GO. Figure 8 shows that the G' values for DX MG/GO and SX MG/GO dramatically increase for inclusion of a small increase of ϕ_{net} compared to the other DX MG and SX MG gels. (Note that 1 wt % of GO is equivalent to a ϕ_{net} increase of 0.05.) The rate of increase was greatest for the DX MG/GO gels (line of best fit shown). These data show that inclusion of GO is a far more effective means to obtain very large increases in modulus compared to increasing the network concentration by simply adding more MG particles. The rate of modulus increase for the DX MG/GO gels is unprecedented for DX MG-based gels, which are a new class of gel.¹ These data also imply that very high G' DX MG-GO gels could be obtained by adding higher C_{GO} values than studied here and, if confirmed by experiment, such an effect may be potentially important in the context of high modulus injectable gels for soft tissue repair of cartilage. Future

work will investigate methods to prepare ultrahigh modulus DX MG/GO gels.

CONCLUSION

This study has investigated the morphology and mechanical properties of colloidal composite gels comprising MG particles and GO. SEM data revealed that the GO sheets were well distributed throughout the matrix. The modulus values (G' and E) for DX MG/GO were found to be proportional to C_{GO} . The modulus values increased by a factor of 5–6 with inclusion of only 1 wt % of GO. The modulus data could be described using the isostrain model of Morris.³⁷ The modulus values for the SX MG/GO were sufficiently large that they could form moldable gels. However, the gels were shear-thinning and were shown to be injectable. The inclusion of GO changed the failure mechanism for the gels to one that resembled that of pure GO gels. Cage breaking was greatly diminished by GO. The ductility of the SX MG/GO and DX MG/GO gels was lower than that for the respective GO-free gels. This was explained in terms of the morphology changes caused by GO, and we propose that the morphologies depicted in Scheme 1 generally apply. The GO sheets were dispersed within MG particle domains (which probably did not involve covalent bonds from GO) for both the SX MG/GO and DX MG/GO gels. GO contributed increasingly to load distribution as the GO concentration increased and behaved as a high surface area, high modulus filler. The results of cell-challenge studies showed that the DX MG/GO_{0.5} gel was not cytotoxic to NP cells. Comparison with data published for GO-free DX MG gels shows that inclusion of GO within DX MG/GO gels provided an unprecedented rate of modulus increase with network volume fraction for this family of colloid gels. The ability to form SX MG/GO gels into self-supporting shapes (Figure 1b) and then cure them using covalent interlinking (Figure 1c) provides the first example of “shape and set” GO-based colloidal composite gels. Considering the good mechanical performance of these novel gel composites, they can be considered as a promising candidate for injectable load-supporting soft tissue repair therapies in the future.

ASSOCIATED CONTENT

Supporting Information

Titration data, SEM and PCS data for the MG particles, TEM, SEM, and Raman spectroscopy data for GO, digital photographs for GO gels, dynamic rheology data for composite gels prepared with and without TEMED, and TGA data for the DX MG/GO composite. This material is available free of charge via the Internet at <http://pubs.acs.org>.

AUTHOR INFORMATION

Notes

The authors declare the following competing financial interest(s): B. Saunders and T. Freemont are the founders of a university spin out company that aims to translate microgel technologies to healthcare applications.

REFERENCES

- (1) Richtering, W.; Saunders, B. R. Gel architectures and their complexity. *Soft Matter* **2014**, *10*, 3695–702.
- (2) Shin, S. R.; Aghaei-Ghareh-Bolagh, B.; Dang, T. T.; Topkaya, S. N.; Gao, X.; Yang, S. Y.; Jung, S. M.; Oh, J. H.; Dokmechi, M. R.; Tang, X. S.; Khademhosseini, A. Cell-laden microengineered and mechanically tunable hybrid hydrogels of gelatin and graphene oxide. *Adv. Mater.* **2013**, *25*, 6385–6391.
- (3) Haraguchi, K.; Takehisa, T. Nanocomposite Hydrogels: A Unique Organic–Inorganic Network Structure with Extraordinary Mechanical, Optical, and Swelling/De-swelling Properties. *Adv. Mater.* **2002**, *14*, 1120–1124.
- (4) Therien-Aubin, H.; Wu, Z. L.; Nie, Z.; Kumacheva, E. Multiple shape transformations of composite hydrogel sheets. *J. Am. Chem. Soc.* **2013**, *135*, 4834–4839.
- (5) Gong, J. Why are double network hydrogels so tough? *Soft Matter* **2010**, *6*, 2583–2590.
- (6) Liu, R.; Milani, A. H.; Freemont, T. J.; Saunders, B. R. Doubly crosslinked pH-responsive microgels prepared by particle interpenetration: swelling and mechanical properties. *Soft Matter* **2011**, *7*, 4696–4704.
- (7) Lyon, L. A.; Meng, Z.; Singh, N.; Sorrell, C. D.; John, A., St Thermoresponsive microgel-based materials. *Chem. Soc. Rev.* **2009**, *38*, 865–874.
- (8) Hoare, T.; Pelton, R. Characterizing charge and crosslinker distributions in polyelectrolyte microgels. *Curr. Opin. Colloid Interface Sci.* **2008**, *13*, 413–428.
- (9) Dai, Z.; Ngai, T. Microgel particles: The structure-property relationships and their biomedical applications. *J. Polym. Sci. A: Polym. Chem.* **2013**, *51*, 2995–3003.
- (10) Saunders, B. R.; Laajam, N.; Daly, E.; Teow, S.; Hu, X.; Stepto, R. Microgels: From responsive polymer colloids to biomaterials. *Adv. Colloid Interface Sci.* **2009**, *147*–*148*, 251–262.
- (11) Hu, J.; Kurokawa, T.; Nakajima, T.; Wu, Z. L.; Liang, S. M.; Gong, J. P. Fracture Process of Microgel-Reinforced Hydrogels under Uniaxial Tension. *Macromolecules* **2014**, *47*, 3587–3594.
- (12) Lehmann, S.; Seiffert, S.; Richtering, W. Spatially resolved tracer diffusion in complex responsive hydrogels. *J. Am. Chem. Soc.* **2012**, *134*, 15963–15969.
- (13) Milani, A. H.; Freemont, A. J.; Hoyland, J. A.; Adlam, D. J.; Saunders, B. R. Injectable Doubly Cross-Linked Microgels for Improving the Mechanical Properties of Degenerated Intervertebral Discs. *Biomacromolecules* **2012**, *13*, 2793–2801.
- (14) Thaiboonrod, S.; Berkland, C.; Milani, A. H.; Ulijn, R.; Saunders, B. R. Poly(vinylamine) microgels: pH-responsive particles with high primary amine contents. *Soft Matter* **2013**, *9*, 3920–3930.
- (15) Thaiboonrod, S.; Milani, A. H.; Saunders, B. R. Doubly crosslinked poly(vinyl amine) microgels: hydrogels of covalently inter-linked cationic microgel particles. *J. Mater. Chem. B* **2014**, *2*, 110–119.
- (16) Chabot, V.; Higgins, D.; Yu, A.; Xiao, X.; Chen, Z.; Zhang, J. A review of graphene and graphene oxide sponge: material synthesis and applications to energy and the environment. *Energy Env. Sci.* **2014**, *7*, 1564–1596.
- (17) Balandin, A. A. Thermal properties of graphene and nanostructured carbon materials. *Nat. Mater.* **2011**, *10*, 569–581.
- (18) Maiti, U. N.; Lee, W. J.; Lee, J. M.; Oh, Y.; Kim, J. Y.; Kim, J. E.; Shim, J.; Han, T. H.; Kim, S. O. 25th Anniversary Article: Chemically Modified/Doped Carbon Nanotubes & Graphene for Optimized Nanostructures & Nanodevices. *Adv. Mater.* **2014**, *26*, 40–67.
- (19) Rafiee, M. A.; Rafiee, J.; Wang, Z.; Song, H.; Yu, Z.-Z.; Koratkar, N. Enhanced Mechanical Properties of Nanocomposites at Low Graphene Content. *ACS Nano* **2009**, *3*, 3884–3890.
- (20) Young, R. J.; Kinloch, I. A.; Gong, L.; Novoselov, K. S. The mechanics of graphene nanocomposites: A review. *Compos. Sci. Technol.* **2012**, *72*, 1459–1476.
- (21) Lerf, A.; He, H.; Forster, M.; Klinowski, J. Structure of Graphite Oxide Revisited. *J. Phys. Chem. B* **1998**, *102*, 4477–4482.
- (22) Dikin, D. A.; Stankovich, S.; Zimney, E. J.; Piner, R. D.; Dommett, G. H.; Evmenenko, G.; Nguyen, S. T.; Ruoff, R. S. Preparation and characterization of graphene oxide paper. *Nature* **2007**, *448*, 457–460.
- (23) Huang, Y.; Zhang, M.; Ruan, W. High-water-content graphene oxide/polyvinyl alcohol hydrogel with excellent mechanical properties. *J. Mater. Chem. A* **2014**, *2*, 10508.

- (24) Cong, H. P.; Wang, P.; Yu, S. H. Highly elastic and superstretchable graphene oxide/polyacrylamide hydrogels. *Small* **2014**, *10*, 448–453.
- (25) Bai, H.; Li, C.; Wang, X.; Shi, G. A pH-sensitive graphene oxide composite hydrogel. *Chem. Commun.* **2010**, *46*, 2376–2378.
- (26) Layek, R. K.; Nandi, A. K. A review on synthesis and properties of polymer functionalized graphene. *Polymer* **2013**, *54*, 5087–5103.
- (27) Liu, J.; Cui, L.; Losic, D. Graphene and graphene oxide as new nanocarriers for drug delivery applications. *Acta Biomater.* **2013**, *9*, 9243–9257.
- (28) Qu, G.; Wang, X.; Liu, Q.; Liu, R.; Yin, N.; Ma, J.; Chen, L.; He, J.; Liu, S.; Jiang, G. The ex vivo and in vivo biological performances of graphene oxide and the impact of surfactant on graphene oxide's biocompatibility. *J. Environ. Sci.* **2013**, *25*, 873–881.
- (29) Chung, C.; Kim, Y.-K.; Shin, D.; Ryoo, S.-R.; Hong, B. H.; Min, D.-H. Biomedical Applications of Graphene and Graphene Oxide. *Acc. Chem. Res.* **2013**, *46*, 2211–2224.
- (30) Bai, H.; Li, C.; Wang, X.; Shi, G. On the Gelation of Graphene Oxide. *J. Phys. Chem. C* **2011**, *115*, 5545–5551.
- (31) Sahu, A.; Choi, W. I.; Tae, G. A stimuli-sensitive injectable graphene oxide composite hydrogel. *Chem. Commun.* **2012**, *48*, 5820–5822.
- (32) Shen, J.; Yan, B.; Li, T.; Long, Y.; Li, N.; Ye, M. Study on graphene-oxide-based polyacrylamide composite hydrogels. *Composites, Part A* **2012**, *43*, 1476–1481.
- (33) Faghihi, S.; Gheysour, M.; Karimi, A.; Salarian, R. Fabrication and mechanical characterization of graphene oxide-reinforced poly(acrylic acid)/gelatin composite hydrogels. *J. Appl. Phys.* **2014**, *115*, 083513.
- (34) Zhao, Q.; An, Q.-F.; Liu, T.; Chen, J.-T.; Chen, F.; Lee, K.-R.; Gao, C.-J. Bio-inspired polyelectrolyte complex/graphene oxide nanocomposite membranes with enhanced tensile strength and ultralow gas permeability. *Polym. Chem.* **2013**, *4*, 4298–4302.
- (35) Liu, R.; Liang, S.; Tang, X.-Z.; Yan, D.; Li, X.; Yu, Z.-Z. Tough and highly stretchable graphene oxide/polyacrylamide nanocomposite hydrogels. *J. Mater. Chem.* **2012**, *22*, 14160–14167.
- (36) Fan, J.; Shi, Z.; Lian, M.; Li, H.; Yin, J. Mechanically strong graphene oxide/sodium alginate/polyacrylamide nanocomposite hydrogel with improved dye adsorption capacity. *J. Mater. Chem. A* **2013**, *1*, 7433.
- (37) Morris, E. R. The effect of solvent partition on the mechanical properties of biphasic biopolymer gels: an approximate theoretical treatment. *Carbohydr. Polym.* **1992**, *17*, 65–70.
- (38) Hummers, W. S.; Offeman, R. E. Preparation of Graphitic Oxide. *J. Am. Chem. Soc.* **1958**, *80*, 1339–1339.
- (39) Dalmont, H.; Pinprayoon, O.; Saunders, B. R. Study of pH-Responsive Microgels Containing Methacrylic Acid: Effects of Particle Composition and Added Calcium. *Langmuir* **2008**, *24*, 2834–2840.
- (40) Xu, C.; Wang, X. Fabrication of flexible metal-nanoparticle films using graphene oxide sheets as substrates. *Small* **2009**, *5*, 2212–2217.
- (41) Wang, X.; Bai, H.; Shi, G. Size Fractionation of Graphene Oxide Sheets by pH-Assisted Selective Sedimentation. *J. Am. Chem. Soc.* **2011**, *133*, 6338–6342.
- (42) Zhu, Y.; Murali, S.; Cai, W.; Li, X.; Suk, J. W.; Potts, J. R.; Ruoff, R. S. Graphene and Graphene Oxide: Synthesis, Properties, and Applications. *Adv. Mater.* **2010**, *22*, 3906–3924.
- (43) Guvendiren, M.; Lu, H. D.; Burdick, J. A. Shear-thinning hydrogels for biomedical applications. *Soft Matter* **2012**, *8*, 260–272.
- (44) Wang, Q.; Wang, L.; Detamore, M. S.; Berkland, C. Biodegradable Colloidal Gels as Moldable Tissue Engineering Scaffolds. *Adv. Mater.* **2008**, *20*, 236–239.
- (45) Vasu, K. S.; Krishnaswamy, R.; Sampath, S.; Sood, A. K. Yield stress, thixotropy and shear banding in a dilute aqueous suspension of few layer graphene oxide platelets. *Soft Matter* **2013**, *9*, 5874–5882.
- (46) Madbouly, S. A.; Otaigbe, J. U. Rheokinetics of Thermal-Induced Gelation of Waterborne Polyurethane Dispersions. *Macromolecules* **2005**, *38*, 10178–10184.
- (47) Goodwin, J. W.; Hughes, R. W. *Rheology for Chemists. An Introduction*; The Royal Society of Chemistry: Cambridge, 2000.
- (48) Dreyer, D. R.; Park, S.; Bielawski, C. W.; Ruoff, R. S. The chemistry of graphene oxide. *Chem. Soc. Rev.* **2010**, *39*, 228–240.
- (49) Godfrin, M. P.; Guo, F.; Chakraborty, I.; Heeder, N.; Shukla, A.; Bose, A.; Hurt, R. H.; Tripathi, A. Shear-directed assembly of graphene oxide in aqueous dispersions into ordered arrays. *Langmuir* **2013**, *29*, 13162–13167.
- (50) Zhou, Z.; Hollingsworth, J. V.; Hong, S.; Cheng, H.; Han, C. C. Yielding behavior in colloidal glasses: comparison between “hard cage” and “soft cage”. *Langmuir* **2014**, *30*, 5739–5746.
- (51) Shao, Z.; Negi, A. S.; Osuji, C. O. Role of interparticle attraction in the yielding response of microgel suspensions. *Soft Matter* **2013**, *9*, 5492–5500.
- (52) Chouquet, A.; Audibert, A.; Moan, M. Linear and non-linear rheological behaviour of cement and silica suspensions. Effect of polymer addition. *Rheol. Acta* **2007**, *46*, 793–802.
- (53) Ma, X.; Li, Y.; Wang, W.; Ji, Q.; Xia, Y. Temperature-sensitive poly(N-isopropylacrylamide)/graphene oxide nanocomposite hydrogels by *in situ* polymerization with improved swelling capability and mechanical behavior. *Eur. Polym. J.* **2013**, *49*, 389–396.
- (54) Kavitha, T.; Kang, I.-K.; Park, S.-Y. Poly(acrylic acid)-Grafted Graphene Oxide as an Intracellular Protein Carrier. *Langmuir* **2013**, *30*, 402–409.
- (55) Costi, J. J.; Stokes, I. A.; Gardner-Morse, M.; Laible, J. P.; Scuffone, H. M.; Iatridis, J. C. Direct measurement of intervertebral disc maximum shear strain in six degrees of freedom: motions that place disc tissue at risk of injury. *J. Biomech.* **2007**, *40*, 2457–2466.
- (56) Lee, J. H.; Ahn, J.; Masuda, M.; Jaworski, J.; Jung, J. H. Reinforcement of a Sugar-Based Bolaamphiphile/Functionalized Graphene Oxide Composite Gel: Rheological and Electrochemical Properties. *Langmuir* **2013**, *29*, 13535–13541.
- (57) Schmidt, S.; Liu, T.; Rütten, S.; Phan, K.-H.; Möller, M.; Richtering, W. Influence of Microgel Architecture and Oil Polarity on Stabilization of Emulsions by Stimuli-Sensitive Core–Shell Poly(N-isopropylacrylamide-co-methacrylic acid) Microgels: Mickering versus Pickering Behavior? *Langmuir* **2011**, *27*, 9801–9806.
- (58) Lally, S.; Cellesi, F.; Freemont, T.; Saunders, B. R. pH-responsive microgels containing hydrophilic crosslinking co-monomers: shell-exploding microgels through design. *Colloid Polym. Sci.* **2011**, *289*, 647–658.